Euwallacea perbrevis (Coleoptera: Curculionidae: Scolytinae), a confirmed pest on *Acacia crassicarpa* in Riau, Indonesia, and a new fungal symbiont; *Fusarium rekanum* sp. nov.

Kira M. T. Lynn[1], Michael J. Wingfield[1], Alvaro Durán[2], Seonju Marincowitz[1], Leonardo S. S. Oliveira[2], Z. Wilhelm de Beer[1] & Irene Barnes[1]

[1]Department of Biochemistry, Genetics and Microbiology (BGM), Forestry and Agricultural Biotechnology Institute (FABI), University of Pretoria, Private Bag X20, Pretoria, 0028, South Africa

[2]Plant Health Program, Research and Development, Asia Pacific Resources International Holdings Ltd. (APRIL), Pangkalan Kerinci 28300, Riau, Indonesia

*Correspondence to Irene Barnes. e-mail: irene.barnes@fabi.up.ac.za

Abstract

Non-native *Acacia* plantations in Indonesia were first reported to be infested by a native ambrosia beetle species, identified as *Euwallacea fornicatus* in 1993. Recently the level of infestation in these plantations by ambrosia beetles has steadily increased. The recent redefinition of the taxonomic parameters of the *Euwallacea fornicatus* species complex has resulted in the identity of the ambrosia beetle species in these plantations becoming unclear. This is also true for their obligate fungal associates. Therefore, the aim of this study was to identify the ambrosia beetle species, as well as its corresponding fungal associate/s, infesting *Acacia crassicarpa* plantations in Riau, Indonesia. Morphological identification and phylogenetic analysis of the mitochondrial cytochrome oxidase c subunit I (COI) gene, revealed that the beetles are *E. perbrevis*, previously a synonym of *E. fornicatus* and commonly referred to as the Tea Shot Hole Borer A (TSHBa). Multi-locus phylogenetic analyses of the fungal associate of *E. perbrevis* revealed a *Fusarium* sp. that is among members of the Ambrosia *Fusarium* Clade (AFC), but that is genetically distinct from other previously identified *Fusarium* symbionts of *Euwallacea* species. This novel fungal species is described here as *Fusarium rekanum* sp. nov.

Keywords: AFC complex; Ambrosia beetle; Euwallacea perbrevis; Fusarium ambrosium; New taxon; Neocosmospora; PHSB

Introduction

Ambrosia beetles are wood-boring mycetophagous insects belonging to the subfamilies Scolytinae and Platypodinae in the larger Curculionidae (Jordal et al. 2011; Hulcr et al. 2015). They are defined by a shared ecological strategy known as fungus farming, with the beetles having obligate nutritional symbioses with fungi (Farrell et al. 2001; Kirkendall et al. 2015). In most ambrosia beetle species, the insects store and transport their fungal associates to and from their natal galleries, in specialised structures known as mycangia (Batra 1963). Once released from the mycangia, the fungi penetrate the xylem tissues of typically dying or occasionally living plant hosts, and grow in the galleries to provide nutrition for the beetles and their offspring (Batra 1963; Mueller et al. 2005).

Ambrosia beetles perform a key role in the ecosystems of their tropical and sub-tropical native ranges by introducing a diverse consortium of fungi into the woody tissues they infest, influencing their rate of decay (Skelton et al. 2019). Many ambrosia beetles and their associated fungi are ecologically constrained to dying trees and usually remain harmless even after establishment in non-native regions. Therefore, they are generally economically inconsequential (Hulcr and Dunn 2011; Ranger et al. 2015; Hulcr et al. 2017). However, several ambrosia beetle species are emerging as prominent pests on trees, particularly in regions where they have been accidently introduced (Hughes et al. 2017; Stouthamer et al. 2017; Gomez et al. 2018).

Ambrosia beetles in the genus *Euwallacea* Hopkins 1915 within the tribe Xyleborini, are particularly successful invaders (Cognato et al. 2015; Stouthamer et al. 2017). This is in part due to their haplodiploid mating system, wide host range and their primary association with *Fusarium* Link species, which can act as both nutritional symbionts and weak phytopathogens (Kasson et al. 2013; O'Donnell et al. 2015). The fusaria associated with *Euwallacea* form a monophyletic group within Clade 3 of the *F. solani* species complex (FSSC), known as the Ambrosia *Fusarium* Clade (AFC, Kasson et al. 2013). Recently, however, Sandoval-Denis et al. (2019) proposed that species in the FSSC, including the AFC species, be placed in the genus *Neocosmospora*.

The AFC comprises of two strongly supported subclades. Clade A includes species that produce curved fusiform septate sporodochial conidia, typical of *Fusarium*. In contrast, most of the species in Clade B produce clavate sporodochial conidia (Kasson et al. 2013). To date, only seven of the 18 species in the AFC have been formally described and include *F. ambrosium* Agnihothr. & Nirenberg (AF-1) (Gadd and Loos 1947), *F. euwallaceae* S. Freeman, Z. Mendel, T. Aoki & O'Donnell (AF-2) (Freeman et al. 2013), *F. oligoseptatum* T. Aoki, M. T. Kasson, S. Freeman, D. M. Geiser & K. O'Donnell (AF-4) (Aoki et al. 2018), *F. kuroshium* F. Na, J.D. Carrillo & Eskalen (AF-12) (Na et al. 2018), *F. floridanum* T. Aoki, Kasson, S. Freeman, Geiser & O'Donnell (AF-3), *F. tuaranense* T. Aoki, Kasson, S. Freeman, Geiser & O'Donnell (AF-5) and *F. obliquiseptatum* T. Aoki, Kasson, S. Freeman, Geiser & O'Donnell (AF-7) (Aoki et al. 2019). Three of these are associated with species in the redefined *E. fornicatus* species complex (Gomez et al. 2018; Smith et al. 2019). The four pests in this redefined complex include *E. perbrevis* Schedl 1951 (Tea Shot Hole Borer Clade a) associated with *F. ambrosium* (AF-1), *E. fornicatior* Eggers 1923 (Tea Shot Hole Borer Clade b) associated with a still unknown symbiont, *E. fornicatus* Schedl 1951 (Polyphagous Shot Hole Borer) associated with *F. euwallaceae* (AF-2), and *E. kuroshio* Gomez & Hulcr 2018 (Kuroshio Shot Hole Borer) associated with *F. kuroshium* (AF-12) (Gomez et al. 2018; Smith et al. 2019).

Species in the *E. fornicatus* complex, along with their AFC associates, are responsible for economic losses to forestry and agricultural industries in various parts of the world (Eskalen et al. 2013; O'Donnell et al. 2016; Na et al. 2018). However, due to previous ambiguous morphological species boundaries, all four species were treated as *E. fornicatus*, despite differences in fungal symbionts, geographic range, and host preference (Gadd and Loos 1947; Freeman et al. 2013; Gomez et al. 2018; Na et al. 2018). This ambiguous level of identification and the revision of the *E. fornicatus* complex, has resulted in confusion regarding the economic importance of these four species.

In Indonesia, *E. fornicatus* has been reported as a pest on *Acacia* spp. where large areas of these exotic trees are planted (Nuhamara, 1993 in Stouthamer et al. 2017). In recent years, there has been a gradual increase in ambrosia beetle infestations within these *Acacia* plantations. This has resulted in significant economic losses to the forestry industry in the region due to tree mortality, a decrease in yield and wood property, and the potential of these insects to vector new aggressive plant pathogens (Roy et al. 2018; Boland and Woodward 2019).

The taxonomic revision of the *E. fornicatus* complex has led to a situation where the identity of the most common ambrosia beetle infesting *Acacia* spp. in Riau, Indonesia is not known. Likewise, the identity of its fungal symbiont/s has not been determined. The aim of this study was therefore to, (1) identify the ambrosia beetles infesting *A. crassicarpa* plantations in Riau, Indonesia, (2) identify the fungal associate/s of the most common beetle species, and (3) determine whether these fungi are pathogens of *A. crassicarpa*.

Materials and methods

Collections of beetle specimens and brood galleries

Plantations of *A. crassicarpa* in Riau, Indonesia, showing heavy ambrosia beetle infestation were identified, and four geographically separated compartments were chosen as collection sites. Based on the infestation scale of Eskalen et al. (2013), three moderately infested living trees [10–30 entry holes] were selected from each site, felled at 50 cm above ground level, and cut into 50 cm logs. These logs were transported to the laboratory where they were dissected, and beetles, along with their galleries, were extracted for morphological and molecular identification.

Fungal isolations

Fungal isolates were either obtained by direct isolation from the mandibular mycangia of mature female beetles (Lynch et al. 2016), or by culturing from the surfaces of the beetle galleries, using methods described by Eskalen et al. (2013). Isolations were performed on Petri dishes containing either potato dextrose agar (PDA; PDA 20 g/L, BD Difco™) or *Fusarium* selective medium (FSM, Leslie and Summerell 2006) amended with 100 µg streptomycin sulphate (Sigma, Steinheim, Germany) to limit the growth of contaminating bacteria and fungi.

For the mycangial extractions, beetles were surface disinfected by submerging individual specimens into Eppendorf tubes containing 70% (v/v) ethanol. Tubes were agitated with a vortex mixer for 10 s before the beetle specimens were removed, rinsed with sterilized distilled water, and air-dried. The beetle heads were separated from the thoracic segments,

macerated or crushed, and were either smeared directly onto the surface of agar or suspended in 200 µL of sterile water in 1.5 mL Eppendorf tubes, shaken for 10 s, and individually pipetted (50 µL) onto the agar and spread using sterile glass rods. The Petri dishes were incubated at 25 °C for 3–5 days to allow for fungal growth. The remaining thoracic and abdominal segments of the beetles were individually stored in 200 µL of 70% (v/v) ethanol for further DNA extractions and identification.

Fungi growing in the beetle galleries were obtained using three different methods as follows: (1) sterile needles were scraped along the gallery surfaces and washed in 200 µL of sterile water. Fifty µL of this suspension was pipetted onto growth medium (FSM and PDA) and spread using sterile glass rods (Kajimura and Hijii 1992); (2) mycelial strands growing inside the beetle galleries, observed using a dissection microscope, were lifted using sterile needles and plated onto FSM and PDA; (3) small pieces of discoloured wood were cut from the edges of the galleries, surface disinfested with 70% (v/v) ethanol and placed on FSM and PDA growth media.

Primary isolations were incubated at 25 °C for 3–5 days to allow for fungal growth. Fungal colonies were sub-cultured onto 2% malt extract agar (MEA: 20 g/L malt extract, 20 g/L agar, Biolab, Midrand, South Africa), amended with 100 µg streptomycin. Five days post sub-culturing, single hyphal tip cultures were made onto MEA, to obtain pure colonies for further identification.

All cultures obtained in this study were deposited in the culture collection (CMW) of the Forestry and Agricultural Biotechnology Institute (FABI), University of Pretoria, Pretoria, South Africa (Table 1, Supplementary Table 1). Representative isolates of the novel species were deposited in the living collection (PPRI) of the South African National Collection of Fungi (NCF), Roodeplaat, South Africa. Dried specimens of sporulating cultures were deposited in the herbarium collection (PREM) of the South African National Collection of Fungi, Roodeplaat, South Africa.

Table 1 Isolates and sequence data used in the phylogenetic analysis of this study

Isolate	Species	Host	Location	GenBank numbers[a]		
				ITS	TEF1-α	RPB2[b]
CMW52862[c,d,e,f]	*Fusarium* sp.	*Euwallacea perbrevis* (TSHBa)	PKU, Indonesia	MN249094	MN249151	MN249137, MN249108
CMW53702[e]	*Fusarium* sp.	*E. perbrevis* (TSHBa)	PKU, Indonesia	MN249095	MN249152	MN249138, MN249109
CMW53701[e]	*Fusarium* sp.	*E. perbrevis* (TSHBa)	PKU, Indonesia	MN249096	MN249153	MN249139, MN249110
CMW53691[e,f]	*Fusarium* sp.	*E. perbrevis* (TSHBa)	PKU, Indonesia	MN249097	MN249154	MN249140, MN249111
CMW53690[e]	*Fusarium* sp.	*E. perbrevis* (TSHBa)	PKU, Indonesia	MN249098	MN249155	MN249141, MN249112
CMW53689[e]	*Fusarium* sp.	*E. perbrevis* (TSHBa)	PKU, Indonesia	MN249099	MN249156	MN249142, MN249113
CMW53688[e,f]	*Fusarium* sp.	*E. perbrevis* (TSHBa)	PKU, Indonesia	MN249100	MN249157	MN249143, MN249114
CMW51756[e]	*Fusarium* sp.	*E. perbrevis* (TSHBa)	PKU, Indonesia	MN249101	MN249158	MN249144, MN249115
CMW51757[e]	*Fusarium* sp.	*E. perbrevis* (TSHBa)	PKU, Indonesia	MN249102	MN249159	MN249145, MN249116
CMW51760[e]	*Fusarium* sp.	*E. perbrevis* (TSHBa)	PKU, Indonesia	MN249103	MN249160	MN249146, MN249117
CMW51764[d,e]	*Fusarium* sp.	*E. perbrevis* (TSHBa)	PKU, Indonesia	MN249104	MN249161	MN249147, MN249118
CMW51765[e]	*Fusarium* sp.	*E. perbrevis* (TSHBa)	PKU, Indonesia	MN249105	MN249162	MN249148, MN249119
CMW51767[e]	*Fusarium* sp.	*E. perbrevis* (TSHBa)	PKU, Indonesia	MN249106	MN249163	MN249149, MN249120
CMW51769[e]	*Fusarium* sp.	*E. perbrevis* (TSHBa)	PKU, Indonesia	MN249107	MN249164	MN249150, MN249121
UCR3641[c]	*F. kuroshium* [AF-12]	*Platanus racemosa*	El Cajon, CA	KX262196	KX262216	KX262256
UCR3644	*F. kuroshium* [AF-12]	*P. racemosa*	El Cajon, CA	KX262197	KX262217	KX262257
UCR3651	*F. kuroshium* [AF-12]	*Euwallacea* sp.	Fallbrook, CA	KX262198	KX262218	KX262258
UCR3653	*F. kuroshium* [AF-12]	*Persea americana*	Bonsall, CA	KX262200	KX262220	KX262260
UCR3654	*F. kuroshium* [AF-12]	*P. americana*	Bonsall, CA	KX262201	KX262221	KX262261
UCR3652	*F. kuroshium* [AF-12]	Unknown	Unknown	KX262199	KX262219	KX262259
UCR4672	*Fusarium* sp. [AF-14]	*Euwallacea* sp.	Taichung, Taiwan	KX262206	KX262226	KX262266
UCR4673	*Fusarium* sp. [AF-16]	*Euwallacea* sp.	Taichung, Taiwan	KX262207	KX262227	KX262267
UCR4674	*Fusarium* sp. [AF-13]	*Euwallacea* sp.	Taichung, Taiwan	KX262208	KX262228	KX262268
UCR4675	*Fusarium* sp. [AF-13]	*Euwallacea* sp.	Taichung, Taiwan	KX262209	KX262229	KX262269
UCR4676	*Fusarium* sp. [AF-17]	*Euwallacea* sp.	Taichung, Taiwan	KX262210	KX262230	KX262270
UCR4677	*Fusarium* sp. [AF-18]	*Euwallacea* sp.	Taichung, Taiwan	KX262211	KX262231	KX262271
UCR4678	*Fusarium* sp. [AF-16]	*Euwallacea* sp.	Taichung, Taiwan	KX262212	KX262232	KX262272

Table 1 continued

Isolate	Species	Host	Location	GenBank numbers[a]		
				ITS	TEF1-α	RPB2[b]
UCR4679	*Fusarium* sp. [AF-15]	*Euwallacea* sp.	Taichung, Taiwan	KX262213	KX262233	KX262273
UCR4680	*Fusarium* sp. [AF-17]	*Euwallacea* sp.	Taichung, Taiwan	KX262214	KX262234	KX262274
UCR4681	*Fusarium* sp. [AF-14]	*Euwallacea* sp.	Taichung, Taiwan	KX262215	KX262235	KX262275
NRRL20438	*F. ambrosium* [AF-1]	*E. perbrevis* (TSHBa)	India	AF178397	AF178332	JX171584
NRRL22231	*F. tuaranense* [AF-5]	*Hevea brasiliensis*	Malaysia	KC691570	KC691542	KC691631, KC691660
NRRL22346	*F. ambrosium* [AF-1]	*E. perbrevis* (TSHBa)	India	EU329669	FJ240350	EU329503
NRRL22468	*F. neocosmosporiellum*	*Arachis hypogaea*	Guinea	DQ094318	AF178349	EU329512
NRRL22643	*Fusarium* sp. [AF-9]	*Xyleborus ferrugineus*	Costa Rica	KC691583	DQ247628	KC691644, KC691673
NRRL32434	*F. lichenicola*	*Homo sapiens*	Germany	DQ094444	DQ246977	EF470161
NRRL46518	*F. tuaranense* [AF-5]	*H. brasiliensis*	Malaysia	KC691571	KC691543	KC691632, KC691661
NRRL54722	*F. euwallaceae* [AF-2]	*Euwallacea* sp.	Israel	JQ038014	JQ038007	JQ038028
NRRL54723	*F. euwallaceae* [AF-2]	*Euwallacea* sp.	Israel	JQ038015	JQ038008	JQ038029
NRRL54724	*F. euwallaceae* [AF-2]	*Euwallacea* sp.	Israel	JQ038016	JQ038009	JQ038030
NRRL54725	*F. euwallaceae* [AF-2]	*Euwallacea* sp.	Israel	JQ038017	JQ038010	JQ038031
NRRL54726	*F. euwallaceae* [AF-2]	*Euwallacea* sp.	Israel	JQ038018	JQ038011	JQ038032
NRRL54727	*F. euwallaceae* [AF-2]	*Euwallacea* sp.	Israel	JQ038019	JQ038012	JQ038033
NRRL62578	*F. oligoseptatum* [AF-4]	*E. validus*	PA (U.S.A.)	KC691565	KC691537	KC691626, KC691655
NRRL62579[c]	*F. oligoseptatum* [AF-4]	*E. validus*	PA (U.S.A.)	KC691566	KC691538	KC691627, KC691656
NRRL62584	*Fusarium* sp. [AF-8]	*Euwallacea* sp.	FL (U.S.A.)	KC691582	KC691554	KC691643, KC691672
NRRL62585	*Fusarium* sp. [AF-8]	*Euwallacea* sp.	FL (U.S.A.)	KC691577	KC691554	KC691638, KC691667
NRRL62590	*Fusarium* sp. [AF-6]	*Euwallacea* sp.	FL (U.S.A.)	KC691574	KC691546	KC691635, KC691664
NRRL62591	*Fusarium* sp. [AF-6]	*Euwallacea* sp.	FL (U.S.A.)	KC691573	KC691545	KC691634, KC691663
NRRL62606	*F. floridanum* [AF-3]	*Euwallacea* sp.	FL (U.S.A.)	KC691561	KC691533	KC691622, KC691651
NRRL62610	*F. obliquiseptatum* [AF-7]	*Euwallacea* sp.	Australia	KC691575	KC691547	KC691636, KC691665
NRRL62611	*F. obliquiseptatum* [AF-7]	*Euwallacea* sp.	Australia	KC691576	KC691548	KC691637, KC691666

Table 1 continued

Isolate	Species	Host	Location	GenBank numbers[a]		
				ITS	TEF1-α	RPB2[b]
NRRL62629	*F. floridanum* [AF-3]	*E. interjectus*	FL (U.S.A.)	KC691564	KC691536	KC691625, KC691654
NRRL62941	*Fusarium* sp. [AF-10]	Unknown	Singapore	KM406633	KM406626	KM406647
NRRL62942	*F. ambrosium* [AF-1]	*Camellia sinensis*	Sri Lanka	KM406631	KM406624	KM406645
NRRL62944	*Fusarium* sp. [AF-11]	*C. sinensis*	Sri Lanka	KM406634	KM406627	KM406648
NRRL66088	*Fusarium* sp. [AF-9]	*Delonix regia*	FL (U.S.A.)	KM406632	KM406632	KM406646
TW1	*Fusarium* sp. [AF-18]	*P. americana*	Danei District, Taiwan	MK432860	MK435437	MK435521
TW2	*Fusarium* sp. [AF-14]	*P. americana*	Danei District, Taiwan	MK432862	MK435439	MK435523
TW4	*Fusarium* sp. [AF-16]	*P. americana*	Danei District, Taiwan	MK432866	MK435443	MK435527
TW15	*Fusarium* sp. [AF-15]	*P. americana*	Danei District, Taiwan	MK432861	MK435438	MK435522
TW25	*Fusarium* sp. [AF-16]	*P. americana*	Danei District, Taiwan	MK432863	MK435440	MK435524
TW34	*Fusarium* sp. [AF-16]	*P. americana*	Danei District, Taiwan	MK432864	MK435441	MK435525
TW37	*Fusarium* sp. [AF-16]	*P. americana*	Danei District, Taiwan	MK432865	MK435442	MK435526
TW40	*Fusarium* sp. [AF-17]	*P. americana*	Danei District, Taiwan	MK432867	MK435444	MK435528
TW43	*F. kuroshium* [AF-12]	*P. americana*	Danei District, Taiwan	MK432868	MK435445	MK435529
TW44	*Fusarium* sp. [AF-18]	*P. americana*	Danei District, Taiwan	MK432869	MK435446	MK435530
TW45	*Fusarium* sp. [AF-15]	*P. americana*	Danei District, Taiwan	MK432870	MK435447	MK435531
TW55	*Fusarium* sp. [AF-18]	*P. americana*	Danei District, Taiwan	MK432871	MK435448	MK435532
TW56	*Fusarium* sp. [AF-14]	*P. americana*	Danei District, Taiwan	MK432872	MK435449	MK435533
UCR5499	*Fusarium* sp. [AF-14]	*Euwallacea* sp.	Danei District, Taiwan	MK432873	MK435450	MK435534
UCR5508	*Fusarium* sp. [AF-16]	*Euwallacea* sp.	Danei District, Taiwan	MK432874	MK435451	MK435535
UCR5509	*Fusarium* sp. [AF-14]	*Euwallacea* sp.	Danei District, Taiwan	MK432875	MK435452	MK435536
UCR5513	*Fusarium* sp. [AF-16]	*Euwallacea* sp.	Danei District, Taiwan	MK432876	MK435453	MK435537
UCR5545	*Fusarium* sp. [AF-17]	*Euwallacea* sp.	Danei District, Taiwan	MK432877	MK435454	MK435538
UCR5546	*Fusarium* sp. [AF-14]	*Euwallacea* sp.	Danei District, Taiwan	MK432878	MK435455	MK435539
UCR5557	*Fusarium* sp. [AF-18]	*Euwallacea* sp.	Danei District, Taiwan	MK432879	MK435456	MK435540
UCR5584	*Fusarium* sp. [AF-13]	*Euwallacea* sp.	Danei District, Taiwan	MK432880	MK435457	MK435541

Table 1 continued

Isolate	Species	Host	Location	GenBank numbers[a]		
				ITS	TEF1-α	RPB2[b]
UCR6394	*Fusarium* sp. [AF-15]	*Euwallacea* sp.	Danci District, Taiwan	MK432881	MK435458	MK435542
UCR6395	*Fusarium* sp. [AF-15]	*Euwallacea* sp.	Danci District, Taiwan	MK432882	MK435459	MK435543
UCR6403	*Fusarium* sp. [AF-13]	*Euwallacea* sp.	Danci District, Taiwan	MK432883	MK435460	MK435544
UCR6405	*Fusarium* sp. [AF-16]	*Euwallacea* sp.	Danci District, Taiwan	MK432884	MK435461	MK435545
UCR6408	*F. kuroshium* [AF-12]	*Euwallacea* sp.	Danci District, Taiwan	MK432885	MK435462	MK435546
UCR6409	*Fusarium* sp. [AF-13]	*Euwallacea* sp.	Danci District, Taiwan	MK432886	MK435463	MK435547
UCR6411	*Fusarium* sp. [AF-18]	*Euwallacea* sp.	Danci District, Taiwan	MK432887	MK435464	MK435548
UCR6414	*Fusarium* sp. [AF-18]	*Euwallacea* sp.	Danci District, Taiwan	MK432888	MK435465	MK435549
UCR6417	*Fusarium* sp. [AF-18]	*Euwallacea* sp.	Danci District, Taiwan	MK432889	MK435466	MK435550
UCR6432	*Fusarium* sp. [AF-13]	*Euwallacea* sp.	Danci District, Taiwan	MK432890	MK435467	MK435551
UCR6436	*Fusarium* sp. [AF-14]	*Euwallacea* sp.	Danci District, Taiwan	MK432891	MK435468	MK435552

PKU Pekanbaru, *CA* California, *PA* Pennsylvania, *FL* Florida

[a]ITS = internal transcribed spacer region; TEF1- α = translation elongation factor 1- α; RPB2 = DNA-directed RNA polymerase II subunit

[b]Two accession numbers correspond to unjoined RPB2-1 and RPB2-2 sequences

[c]Type-species

[d]Isolates used in the pathogenicity test

[e]Indonesian isolates collected and sequenced in this study

[f]Isolates used in morphological descriptions and growth studies

DNA extraction and PCR

Beetle specimens

Specimens were initially characterised based on morphology and grouped utilising similarities in body form and declivital sculpturing. A subset of 30 individual specimens was selected for DNA extraction, including a representative from each morphological group. DNA was extracted from the beetle wings and legs using the prepGEM™ Universal DNA extraction kit [Zygem, Biocom Africa (Pty) Ltd.], following the manufacturers protocol, except that the final product was not diluted. The extracted DNA was subjected to PCR amplification of the mitochondrial cytochrome oxidase c subunit I gene (COI), using the primer pair LCO1490 and HCO2198 (Folmer et al. 1994). Each PCR reaction mixture consisted of 0.2 µL FastStart™ Taq DNA Polymerase (Roche), 10.8 µL sterile DNase-free water, 1 µL of 10 mM both forward and reverse primer, 3 µL of 25 mM $MgCl_2$, 2.5 µL 10 × PCR Buffer and 4 µL of DNA template, for a 25 µL total reaction mixture. PCR amplification was carried out on a Bio-Rad iCycler thermocycler (BIO-RAD, Hercules, CA, USA), programmed for an initial denaturing step of 95 °C for 7 min; followed by 35 cycles of 94 °C for 30 s, 58 °C for 30 s and 72 °C for 1 min; ending with a final extension of 7 min at 72 °C. Amplification was confirmed by staining 2 µL PCR product with 2 µL GelRed™

Nucleic Acid Gel stain (Biotium, Hayward, CA, USA), and separating them on a 2% agarose gel, followed by visualization under UV light.

Fungal isolates

Three-day-old cultures of all isolates resembling *Fusarium* spp., were used for DNA extraction using Prepman® Ultra Sample Preparation Reagent (Thermo Fisher Scientific, Waltham, MA, USA) following the manufacturer's protocol. PCR amplification was performed for: the ribosomal internal transcribed spacer region and the domains D1 and D2, at the 5′ end of the nuclear large subunit (ITS 1-5.8S-ITS2 + LSU rDNA), using the primers ITS4/ITS5 (White et al. 1990) and NL1/NL4 (Kurtzman and Robnett 1997), respectively; the translation elongation factor 1-α (TEF1-α) using the primers EF1/EF2 (O'Donnell et al. 1998) and the RNA polymerase subunit II (RPB2), using the primer pairs 5F2/7CR (RPB2-1) and 7CF/11AR (RPB2-2) (O'Donnell et al. 2007). PCR amplifications were performed in 13 µL reactions containing 2.5 µL 5 × MyTaq buffer (Bioline, London, UK), 0.25 µL MyTaq DNA polymerases (Bioline), 1 µL DNA template, 0.5 µL of each primer (10 mM), and 8.25 µL of sterile deionized water. PCR was performed for each primer pair using published cycling parameters (White et al. 1990; O'Donnell and Cigelnik 1997; Jacobs et al. 2004; O'Donnell et al. 2007). Amplification of products was confirmed with gel electrophoresis as stated above. PCR amplification of the RNA polymerase subunit I (RPB1), using the primer pairs F5/R8 (RPB1-1) and F7/G2R (RPB1-2) (O'Donnell et al. 2010), was unsuccessful across all isolates.

DNA sequencing

PCR products were purified using 6% Sephadex G-50 columns following the manufacturer's protocol (Sigma, Aldrich Germany). Products were sequenced in both directions in 12 µL reactions, using the same primers used for PCR amplification. The reaction mixture contained 1 µL BigDye® Terminator v. 3.1 ready reaction mixture (Perkin-Elmer, Warrington, UK), 1 µL sequencing buffer, 1 µL of either the forward or reverse primer (10 mM) for each gene region and 1.5 µL cleaned PCR product. The thermal cycling conditions included 25 cycles of 10 s at 96 °C, 5 s at 55 °C and 4 min at 60 °C. Sequencing products were cleaned using 6% Sephadex G-50 columns and dried in an Eppendorf 5301 vacuum concentrator at 60 °C for 5 min. Sequencing was performed at the sequencing facility of the University of Pretoria, on an ABI PRISM™ 3500xl Auto-sequencer (Applied Biosystems, Foster City, CA, USA). The forward and reverse sequencing reads were assembled into contigs using CLC Bio Main Workbench v. 6 (CLC Bio, www.clcbio.com), and from which consensus sequences were extracted and exported for phylogenetic analysis.

Phylogenetic analyses

Beetle specimens

A preliminary identity for the beetle specimens was obtained by performing a nucleotide BLAST of the COI sequences against the NCBI GenBank database (http://www-ncbi-nlm-nih-gov.uplib.idm.oclc.org). Based on the results, sequences of closely related taxa were downloaded to compile datasets for phylogenetic analyses. Additionally, sequences available from previous studies (Gomez et al. 2018; Na et al. 2018), were also incorporated into the datasets. Sequences were aligned in MEGA v. 7 (Kumar et al. 2016), using the inbuilt MUSCLE alignment software (Edgar 2004), and manually inspected and adjusted.

Genealogical relationships among individual beetles were reconstructed using maximum likelihood (ML) analyses, which were performed on the online CIPRES Science Gateway v 3.3 platform (Miller et al. 2010), using the online RAxML-HPC BlackBox v. 8.2.10 tool (Stamatakis 2014). Maximum likelihood analyses were carried out using the GTRGAMMA + I substitution model with all other parameters set to default. A non-parametric analysis of the sequence data with 1000 bootstrap replicates provided statistical support for the branches of the generated ML trees. *Ambrosiophilus sexdentatus* (HM06405) was used to root the ML analysis as suggested by Gomez et al. (2018).

The DNA for the representative specimens sequenced in this study are stored in the Entomological database of the Forestry and Agricultural Biotechnology Institute (FABI), University of Pretoria, South Africa. All additional specimens collected in this study are stored in 70% (v/v) ethanol at 5 °C at the Forestry and Agricultural Biotechnology Institute (FABI), University of Pretoria, South Africa.

Fusarium isolates

Initial BLAST searches of the resulting translation elongation factor 1-α (TEF1-α) sequences, against the NCBI GenBank database, were performed to putatively identify fungal isolates. As with the beetles, sequences of closely related taxa were then downloaded, along with those used in previous studies (Kasson et al. 2013; O'Donnell et al. 2015; Carrillo et al. 2019) (Table 1), to construct datasets for phylogenetic analyses. DNA sequences for the ITS, TEF1-α and RPB2 gene regions (Table 1), from 14 selected isolates of a *Fusarium* sp. obtained in this study, were individually aligned with each respective gene dataset in MEGA v. 7, following the same procedure as stated above. The individual datasets were subsequently combined using FASconCAT-G (Kück and Longo 2014).

Using the concatenated dataset, a maximum likelihood (ML) multigene phylogeny was constructed. jModelTest2 (Darriba et al. 2015) was used on the combined dataset to determine the best substitution model. Maximum likelihood tree construction was performed using PhyML v. 3.1 (Guindon et al. 2010), with the following criteria: proportion of non-variable sites 0.484, gamma shape 0.311 and the number of substitution sites set to 6. The starting tree was obtained using a BioNJ approach and the branch swopping strategy was set to select the best NNI algorithm. Statistical support for the branches in the ML trees was obtained by performing 1000 bootstrap replicates. *Fusarium neocosmosporiellum* (NRRL 22468) and *Fusarium lichenicola* (NRRL 32434) were used as the outgroups based on previous studies (Kasson et al. 2013; O'Donnell et al. 2015).

Morphological characterization of *Fusarium* spp.

To investigate the morphological characters of the fungus, three representative isolates (CMW 52862, CMW 53688 and CMW 53691) were selected for the study. Fourteen-day-old cultures grown on PDA and synthetic low-nutrient agar (SNA: 0.2 g glucose, 0.2 g sucrose, 1 g KH_2PO_4, 1 g KNO_3, 0.5 g $MgSO_4$, 7 H_2O, 0.5 g KCl, 20 g Difco agar per litre; Leslie and Summerell 2006) in darkness, under continuous UV light or under an ambient daylight photoperiod, at ambient room temperature (23–25 °C), were used to evaluate the microscopic characters considered by Aoki et al. (2005) and Freeman et al. (2013). Microscope slides were prepared for each isolate with structures mounted in water and 25–50 measurements were recorded for each characteristic, using a Nikon H550L microscope (Nikon, Yokohama, Japan). Means, standard deviation, standard error, max, and min values of the microscopic

characters were calculated and presented as minimum–(mean minus standard deviation)–mean–(mean plus standard deviation)–maximum.

To determine optimum growth conditions, colony growth rate was determined for each representative isolate of the *Fusarium* sp. Three replicates of each isolate were assessed at temperatures ranging from 10 to 35 °C at 5 °C intervals grown in the dark. Agar plugs (5 mm) were cut from the edges of 1-week-old cultures and placed at the centres of 90 mm Petri dishes containing PDA. Two measurements of colony diameter perpendicular to each other were made, every day for 10 days, after which averages were determined. After 14 days, the cultures grown at 25 °C in the dark were used to characterize colony colour (surface and reverse), odour and colony morphology. Colony colours (surface and reverse) were described using the colour charts of Rayner (1970).

Pathogenicity assay

To determine the pathogenicity of the *Fusarium* sp. on *A. crassicarpa*, two isolates (Treatment 1 = CMW 52862 and Treatment 2 = CMW 51764) were selected and each inoculated into the stems of 16, seven-to-eight-month-old, *A. crassicarpa* trees. The fungal cultures were grown on PDA for 7 days at 25 °C, and 6 mm agar plugs were cut from the leading edges of the cultures using a sterilized cork borer. The same size cork borer was flame-sterilized and used to make wounds in the stems of the trees, removing the phloem tissues to expose the cambium. The agar plugs were then placed in the wounds, mycelium-side facing the cambium and the inoculation sites were covered with Parafilm® (Bemis NA) and sealed with adhesive tape. Sixteen trees were inoculated in the same manner with sterile PDA to serve as controls.

Inoculations were inspected after 30 days, by removing the bark to assess lesion development. Lesion lengths were measured from the edges of visible discolouration in the wood. A Shapiro–Wilk test and Levene's test were performed in R (v. 3.2.3), to assess whether the data was normally distributed and homogeneous, respectively. The data were subsequently raised to the power of − 0.5 in R to obtain a normal distribution. To test the difference between lesion length of the different treatments and the controls, an analysis of variance (ANOVA) using the agricolae package in R was performed (de Mendiburu 2019). Ad hoc Tukey's bootstrap test was performed with the log-transformed data at $\alpha = 0.05$, to determine whether there were significant differences between the individual isolates compared to the control and between the isolates themselves. All plots were made using ggplot in the package R tidyverse (Wickham 2017).

To test Koch's postulates, xylem samples from the margins of the lesions were taken to attempt re-isolation of the inoculated fungi. Small pieces of the xylem tissue, including those from the control plants, were plated onto PDA and FSM amended with 100 µg streptomycin, and incubated at 25 °C for 5 days. The resulting isolates were identified using DNA sequences for the translation elongation factor 1-α (TEF1-α) as described above. Resulting sequences were aligned to the original isolate sequence data in CLC Bio Main Workbench v. 6 (CLC Bio, www.clcbio.com), to confirm the presence of the inoculated fungi.

Results

PCR amplification and sequencing

Beetle specimens

In total, 51 beetle galleries were extracted from infested trees (Fig. 1a), and 61 beetle specimens were collected. Based on preliminary morphological characterisation, five different beetle taxa were identified. Successful PCR amplification of the COI gene was carried out for all beetle specimens, with a resulting amplicon length of approximately 800 bp.

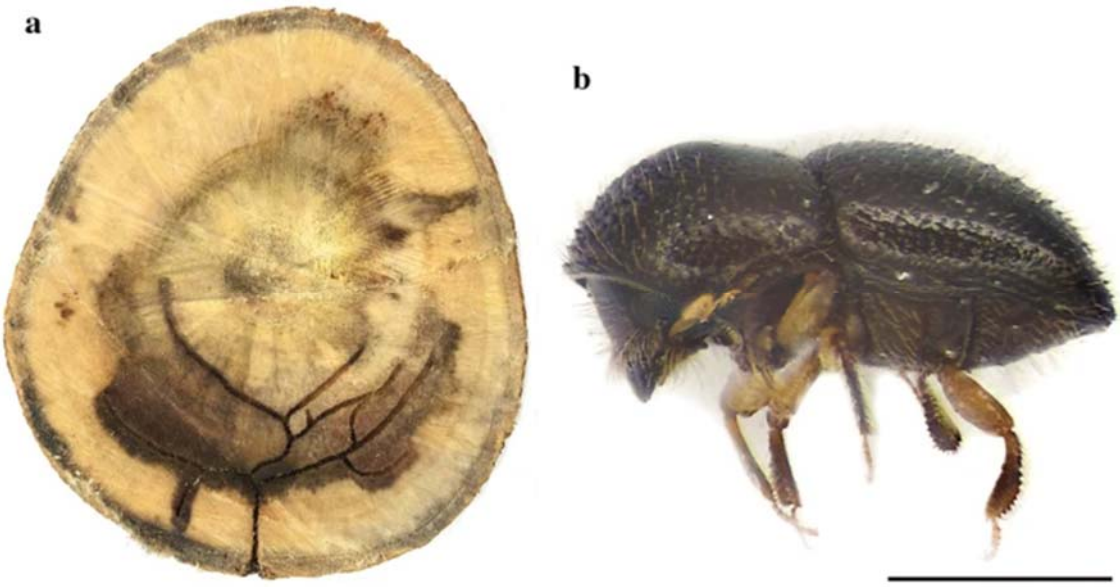

Fig. 1. *Euwallacea perbrevis* and its brood gallery. **a** Brood gallery of *Euwallacea perbrevis* (TSHBa) in two-year-old *A. crassicarpa*. **b** Mature female *Euwallacea perbrevis* (TSHBa) beetle collected from infested *Acacia crassicarpa* in Indonesia. Scale bar = 1.0 mm

Morphological characters, such as body size (Fig. 1b), and ML phylogenetic analysis of the DNA sequence data (Fig. 2), showed that *Euwallacea perbrevis* (TSHBa) was the most abundantly collected beetle species, representing 49% of the samples. The 15 individual TSHBa beetles sequenced represented two distinct COI haplotypes (Fig. 2), one of which is novel. These haplotypes differed from each other by 6 bp, but both grouped into the same clade with other specimens collected from Indonesia (Gomez et al. 2018), with a 100% bootstrap support. The novel haplotype, represented by seven individuals, differed by 4 bp to its closest lineage (MH276909), isolated from East Java, Indonesia. The second haplotype was represented by eight individuals and grouped with a previously identified specimen from East Java, Indonesia (MH276910) with a bootstrap support of 89% (Gomez et al. 2018). The aligned dataset for COI (94 taxa, 569 characters) was deposited in TreeBASE (http://purl.org/phylo/treebase/phylows/study/TB2:S25628) and all sequences obtained for the TSHBa beetle specimens in this study were deposited in GenBank (Table 2).

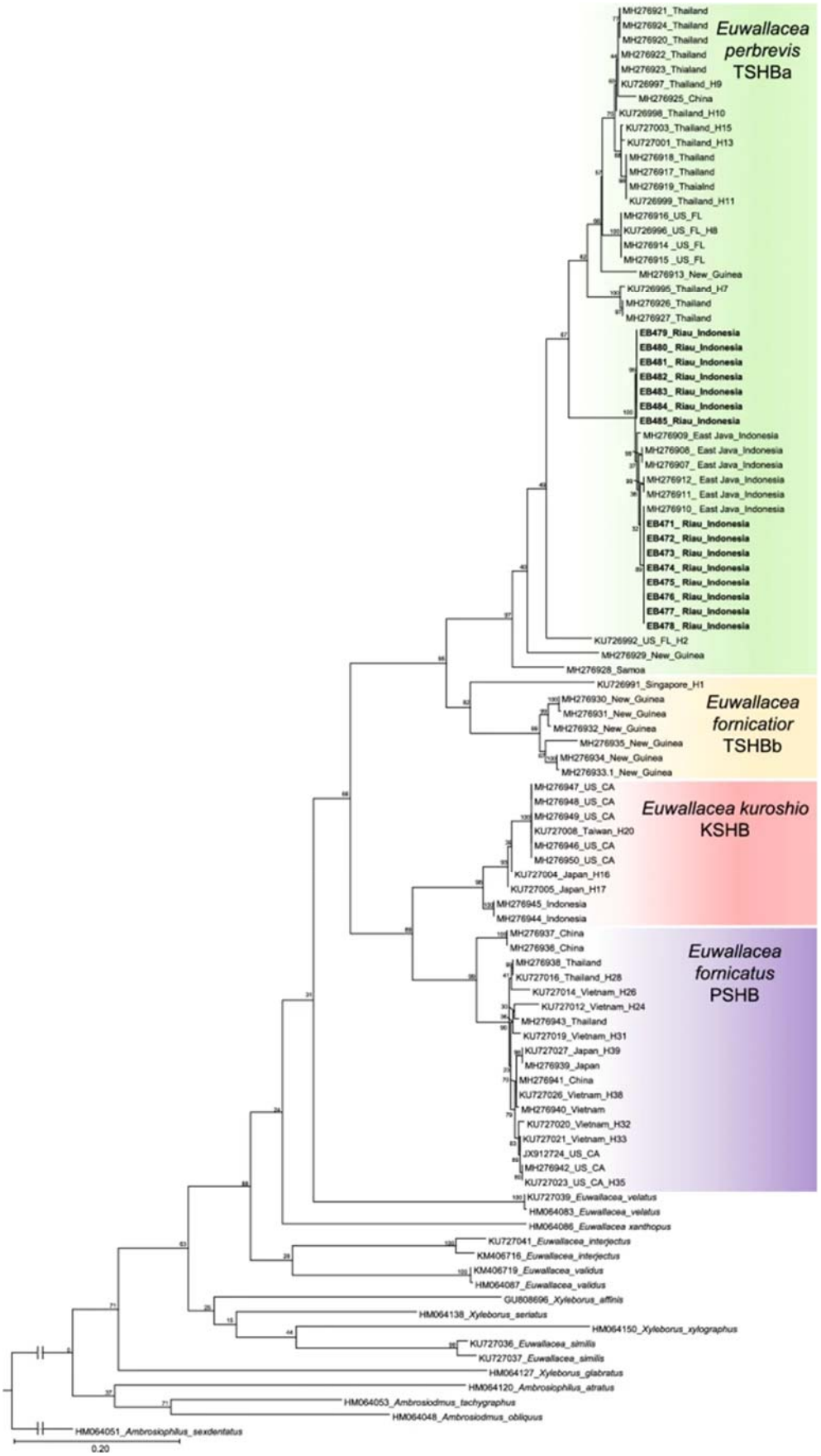
Euwallacea perbrevis TSHBa
MH276921_Thailand
MH276924_Thailand
MH276920_Thailand
MH276922_Thailand
MH276923_Thialand
KU726997_Thailand_H9
MH276925_China
KU726998_Thailand_H10
KU727003_Thailand_H15
KU727001_Thailand_H13
MH276918_Thailand
MH276917_Thailand
MH276919_Thaialnd
KU726999_Thailand_H11
MH276916_US_FL
KU726996_US_FL_H8
MH276914 _US_FL
MH276915 _US_FL
MH276913_New_Guinea
KU726995_Thailand_H7
MH276926_Thailand
MH276927_Thailand
EB479_Riau_Indonesia
EB480_ Riau_Indonesia
EB481_ Riau_Indonesia
EB482_ Riau_Indonesia
EB483_ Riau_Indonesia
EB484_ Riau_Indonesia
EB485_Riau_Indonesia
MH276909_East Java_Indonesia
MH276908_ East Java_Indonesia
MH276907_ East Java_Indonesia
MH276912_ East Java_Indonesia
MH276911_ East Java_Indonesia
MH276910_ East Java_Indonesia
EB471_ Riau_Indonesia
EB472_ Riau_Indonesia
EB473_ Riau_Indonesia
EB474_ Riau_Indonesia
EB475_ Riau_Indonesia
EB476_ Riau_Indonesia
EB477_ Riau_Indonesia
EB478_ Riau_Indonesia
KU726992_US_FL_H2
MH276929_New_Guinea
MH276928_Samoa
KU726991_Singapore_H1
Euwallacea fornicatior TSHBb
MH276930_New_Guinea
MH276931_New_Guinea
MH276932_New_Guinea
MH276935_New_Guinea
MH276934_New_Guinea
MH276933.1_New_Guinea
Euwallacea kuroshio KSHB
MH276947_US_CA
MH276948_US_CA
MH276949_US_CA
KU727008_Taiwan_H20
MH276946_US_CA
MH276950_US_CA
KU727004_Japan_H16
KU727005_Japan_H17
MH276945_Indonesia
MH276944_Indonesia
Euwallacea fornicatus PSHB
MH276937_China
MH276936_China
MH276938_Thailand
KU727016_Thailand_H28
KU727014_Vietnam_H26
KU727012_Vietnam_H24
MH276943_Thailand
KU727019_Vietnam_H31
KU727027_Japan_H39
MH276939_Japan
MH276941_China
KU727026_Vietnam_H38
MH276940_Vietnam
KU727020_Vietnam_H32
KU727021_Vietnam_H33
JX912724_US_CA
MH276942_US_CA
KU727023_US_CA_H35
KU727039_Euwallacea_velatus
HM064083_Euwallacea_velatus
HM064086_Euwallacea xanthopus
KU727041_Euwallacea_interjectus
KM406716_Euwallacea_interjectus
KM406719_Euwallacea_validus
HM064087_Euwallacea_validus
GU808696_Xyleborus_affinis
HM064138_Xyleborus_seriatus
HM064150_Xyleborus_xylographus
KU727036_Euwallacea_similis
KU727037_Euwallacea_similis
HM064127_Xyleborus_glabratus
HM064120_Ambrosiophilus_atratus
HM064053_Ambrosiodmus_tachygraphus
HM064048_Ambrosiodmus_obliquus
HM064051_Ambrosiophilus_sexdentatus
0.20

Fig. 2. Phylogenetic tree based on maximum likelihood (ML) analysis of COI gene sequences for various ambrosia beetle species in the *Euwallacea fornicatus* sensu lato complex (Gomez et al. 2018). Specimens in bold were sequenced in this study and represented two distinct haplotypes. Both haplotypes grouped with the other specimens collected from Indonesia with 100% bootstrap support. One novel haplotype represented by seven individuals was supported with a bootstrap of 95%, whereas the second haplotype grouped with other previously identified specimen from Indonesia (MH276910) and contained eight individuals with a bootstrap support of 89%. *Ambrosiophilus sexdentatus* (HM064051) represents the outgroup

Table 2 Descriptions and sequences of specimens collected in this study and used for phylogenetic analysis

Specimen	Genetic lineage	Country	Locality	GenBank accession COI gene region
EB471	*Euwallacea perbrevis* (TSHBa)	Indonesia	Pekanbaru, Riau	MN249122
EB472	*E. perbrevis* (TSHBa)	Indonesia	Pekanbaru, Riau	MN249123
EB473	*E. perbrevis* (TSHBa)	Indonesia	Pekanbaru, Riau	MN249124
EB474	*E. perbrevis* (TSHBa)	Indonesia	Pekanbaru, Riau	MN249125
EB475	*E. perbrevis* (TSHBa)	Indonesia	Pekanbaru, Riau	MN249126
EB476	*E. perbrevis* (TSHBa)	Indonesia	Pekanbaru, Riau	MN249127
EB477	*E. perbrevis* (TSHBa)	Indonesia	Pekanbaru, Riau	MN249128
EB478	*E. perbrevis* (TSHBa)	Indonesia	Pekanbaru, Riau	MN249129
EB479	*E. perbrevis* (TSHBa)	Indonesia	Pekanbaru, Riau	MN249130
EB480	*E. perbrevis* (TSHBa)	Indonesia	Pekanbaru, Riau	MN249131
EB481	*E. perbrevis* (TSHBa)	Indonesia	Pekanbaru, Riau	MN249132
EB482	*E. perbrevis* (TSHBa)	Indonesia	Pekanbaru, Riau	MN249133
EB483	*E. perbrevis* (TSHBa)	Indonesia	Pekanbaru, Riau	MN249134
EB484	*E. perbrevis* (TSHBa)	Indonesia	Pekanbaru, Riau	MN249135
EB485	*E. perbrevis* (TSHBa)	Indonesia	Pekanbaru, Riau	MN249136

Morphological identification using the online, Southeast Asia ambrosia beetles identification resource (http://idtools.org/id/wbb/sea-ambrosia/index.php), and BLAST results of COI sequences of representative individuals, identified the remaining three beetle taxa as: *Xyleborinus exiguus* Wood & Bright 1992 (syn. *X. perexiguus*; 97% identity to HM064109), *Xylosandrus crassiusculus* Motschulsky 1866 (99% identity to KX035196) and *E. similis* Ferrari 1867 (94% identity to KU727036). The remaining beetle was identified as *Hypothenemus eruditus* Westwood 1836 (99% identity to KY800193), using the BLAST results of COI sequences and the online site 'Featured Creatures' (http://entnemdept.ufl.edu/creatures/). With the exception of *H. eruditus*, these are all ambrosia beetles that reside in the tribe Xyleborini. *Hypothenemus eruditus* is a true weevil in the Cryphalini.

Fungal isolates

Nighty-nine fungal isolates were obtained from the beetle mycangia and brood galleries. These included 18 different fungal genera (Supplementary Table 1), of which *Fusarium* spp. were most commonly isolated across all isolation methods. Due to the fact that beetles in the *E. fornicatus* complex commonly have an association with *Fusarium* spp. (Kasson et al. 2013), the *Fusarium* isolates obtained from the selected sub-population of *E. perbrevis* became the focus of this study.

The second most abundant fungi isolated were Hypocrealean fungi. In addition, a single isolate of a *Graphium* sp. and *Paracremonium* sp. were collected, both of which have previously been identified as community members associated with other species in the *E. fornicatus* complex (Lynch et al. 2016; Na et al. 2018). A single isolate was also collected

that is genetically very similar to *Ambrosiella roeperi* T.C. Harr. & McNew (99% identity to NR154684), the mycangial symbiont of *X. crassiusculus* (Harrington et al. 2014).

A collection of 14 isolates of a *Fusarium* sp., originating from both mycangial isolations and isolations from the beetle galleries, was selected for further phylogenetic analysis using the ITS-LSU, TEF1-α and RPB 2 datasets. The amplicon lengths for the ITS-LSU, TEF1-α and RPB 2 gene regions were approximately 1100 bp, 700 bp and 1400 bp, respectively. All sequences obtained for the 14 *Fusarium* sp. isolates in this study were deposited in GenBank (Table 1). The aligned sequences for the ITS (89 taxa, 393 characters), RPB 2 (89 taxa, 1145 characters), TEF1-α (89 taxa, 278 characters), and the combined ITS, RPB2 and TEF1-α (89 taxa, 1815 characters) datasets, were deposited in TreeBASE (http://purl.org/phylo/treebase/phylows/study/TB2:S25627). The best model of evolution for the combined dataset was identified as TIM+I+G.

Maximum likelihood phylogenetic analyses of the individual TEF1-α (Supplementary Fig. 1) and RPB2 (Supplementary Fig. 2) datasets, as well as the combined ITS, RPB 2 and TEF1-α (Fig. 3) dataset, consistently showed that the isolates from both the *E. perbrevis* mycangia and brood galleries, represented a distinct and previously undescribed species. This new taxon, which had high bootstrap support in all analyses, formed a new AFC lineage in subclade B, identified here as AF-19.

RPB 2 was the most informative gene region, providing high bootstrap support for eight of the 19 AFC species, including the new lineage (AF-19) emerging from this study (Supplementary Fig. 2). In contrast, bootstrap analysis of the ITS rDNA provided the weakest signal and resolved only three of the 19 AFC species (Supplementary Fig. 3). As has been found previously, the combined analysis (ITS, RPB2 and TEF1-α), provided the strongest support for the evolutionary relationships within members of the AFC, with high bootstrap support for 11 of the 19 AFC species. In the combined analysis, a total of 13 out of 19 AFC members were resolved with the exceptions of AF-12, AF-13, AF-14, AF-15, AF-17 and AF-18 (Fig. 3). Thus, phylogenetic analyses across two of the three gene regions consistently supported the presence of a previously unknown *Fusarium* lineage (AF-19), distinct from all other previously identified clades for *Fusarium* spp. associated with ambrosia beetles.

The topology of the ML phylogram presented in this study based on the combined data set, differed slightly from that in a previous study by Carrillo et al. (2019). Unlike their analyses, we excluded the RPB 1 gene region as we were unable to successfully amplify this gene region. Major groupings within both analyses were, however, similar. Bootstrap support for the two AFC clades (Clade A and B of Kasson et al. 2013) was well supported (Fig. 3). However, support for the backbone of the AFC Clade B, in which our isolates from *E. perbrevis* grouped, was weak with 11 nodes having a bootstrap value below 50%.

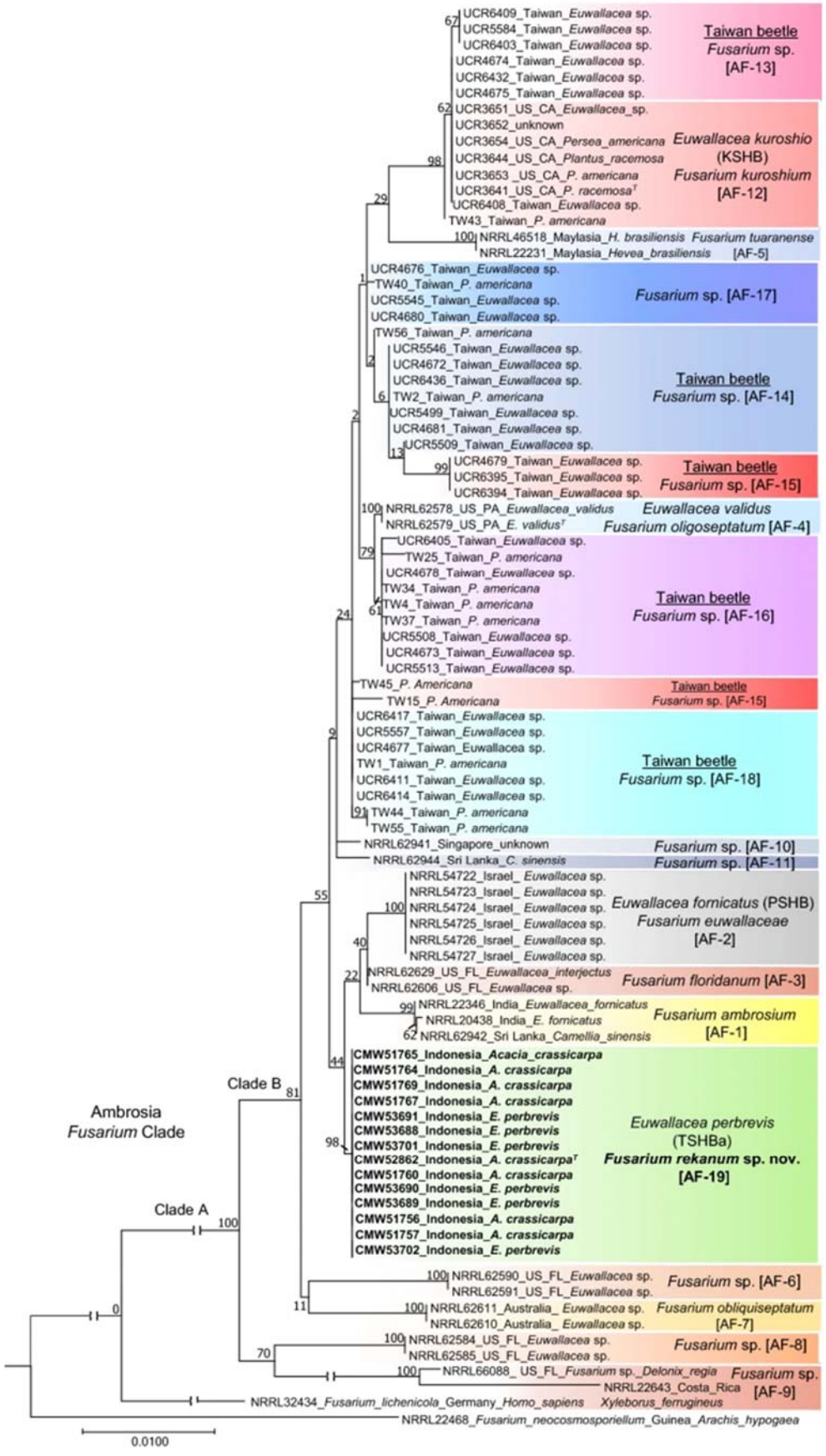
UCR6409_Taiwan_Euwallacea sp.
UCR5584_Taiwan_Euwallacea sp.
UCR6403_Taiwan_Euwallacea sp.
UCR4674_Taiwan_Euwallacea sp.
UCR6432_Taiwan_Euwallacea sp.
UCR4675_Taiwan_Euwallacea sp.
Taiwan beetle
Fusarium sp.
[AF-13]
UCR3651_US_CA_Euwallacea_sp.
UCR3652_unknown
UCR3654_US_CA_Persea_americana
UCR3644_US_CA_Plantus_racemosa
UCR3653 _US_CA_P. americana
UCR3641_US_CA_P. racemosaT
UCR6408_Taiwan_Euwallacea sp.
TW43_Taiwan_P. americana
Euwallacea kuroshio
(KSHB)
Fusarium kuroshium
[AF-12]
NRRL46518_Maylasia_H. brasiliensis
NRRL22231_Maylasia_Hevea_brasiliensis
Fusarium tuaranense
[AF-5]
UCR4676_Taiwan_Euwallacea sp.
TW40_Taiwan_P. americana
UCR5545_Taiwan_Euwallacea sp.
UCR4680_Taiwan_Euwallacea sp.
Fusarium sp. [AF-17]
TW56_Taiwan_P. americana
UCR5546_Taiwan_Euwallacea sp.
UCR4672_Taiwan_Euwallacea sp.
UCR6436_Taiwan_Euwallacea sp.
TW2_Taiwan_P. americana
UCR5499_Taiwan_Euwallacea sp.
UCR4681_Taiwan_Euwallacea sp.
UCR5509_Taiwan_Euwallacea sp.
Taiwan beetle
Fusarium sp. [AF-14]
UCR4679_Taiwan_Euwallacea sp.
UCR6395_Taiwan_Euwallacea sp.
UCR6394_Taiwan_Euwallacea sp.
Taiwan beetle
Fusarium sp. [AF-15]
NRRL62578_US_PA_Euwallacea_validus
NRRL62579_US_PA_E. validusT
Euwallacea validus
Fusarium oligoseptatum [AF-4]
UCR6405_Taiwan_Euwallacea sp.
TW25_Taiwan_P. americana
UCR4678_Taiwan_Euwallacea sp.
TW34_Taiwan_P. americana
TW4_Taiwan_P. americana
TW37_Taiwan_P. americana
UCR5508_Taiwan_Euwallacea sp.
UCR4673_Taiwan_Euwallacea sp.
UCR5513_Taiwan_Euwallacea sp.
Taiwan beetle
Fusarium sp. [AF-16]
TW45_P. Americana
TW15_P. Americana
Taiwan beetle
Fusarium sp. [AF-15]
UCR6417_Taiwan_Euwallacea sp.
UCR5557_Taiwan_Euwallacea sp.
UCR4677_Taiwan_Euwallacea sp.
TW1_Taiwan_P. americana
UCR6411_Taiwan_Euwallacea sp.
UCR6414_Taiwan_Euwallacea sp.
TW44_Taiwan_P. americana
TW55_Taiwan_P. americana
Taiwan beetle
Fusarium sp. [AF-18]
NRRL62941_Singapore_unknown
Fusarium sp. [AF-10]
NRRL62944_Sri Lanka_C. sinensis
Fusarium sp. [AF-11]
NRRL54722_Israel_ Euwallacea sp.
NRRL54723_Israel_ Euwallacea sp.
NRRL54724_Israel_ Euwallacea sp.
NRRL54725_Israel_ Euwallacea sp.
NRRL54726_Israel_ Euwallacea sp.
NRRL54727_Israel_ Euwallacea sp.
Euwallacea fornicatus (PSHB)
Fusarium euwallaceae
[AF-2]
NRRL62629_US_FL_Euwallacea_interjectus
NRRL62606_US_FL_Euwallacea sp.
Fusarium floridanum [AF-3]
NRRL22346_India_Euwallacea_fornicatus
NRRL20438_India_E. fornicatus
NRRL62942_Sri Lanka_Camellia_sinensis
Fusarium ambrosium
[AF-1]
CMW51765_Indonesia_Acacia_crassicarpa
CMW51764_Indonesia_A. crassicarpa
CMW51769_Indonesia_A. crassicarpa
CMW51767_Indonesia_A. crassicarpa
CMW53691_Indonesia_E. perbrevis
CMW53688_Indonesia_E. perbrevis
CMW53701_Indonesia_E. perbrevis
CMW52862_Indonesia_A. crassicarpaT
CMW51760_Indonesia_A. crassicarpa
CMW53690_Indonesia_E. perbrevis
CMW53689_Indonesia_E. perbrevis
CMW51756_Indonesia_A. crassicarpa
CMW51757_Indonesia_A. crassicarpa
CMW53702_Indonesia_E. perbrevis
Euwallacea perbrevis
(TSHBa)
Fusarium rekanum sp. nov.
[AF-19]
NRRL62590_US_FL_Euwallacea sp.
NRRL62591_US_FL_Euwallacea sp.
Fusarium sp. [AF-6]
NRRL62611_Australia_ Euwallacea sp.
NRRL62610_Australia_ Euwallacea sp.
Fusarium obliquiseptatum
[AF-7]
NRRL62584_US_FL_Euwallacea sp.
NRRL62585_US_FL_Euwallacea sp.
Fusarium sp. [AF-8]
NRRL66088_ US_FL_Fusarium sp._Delonix_regia
NRRL22643_Costa_Rica
Fusarium sp.
[AF-9]
Xyleborus_ferrugineus
NRRL32434_Fusarium_lichenicola_Germany_Homo_sapiens
NRRL22468_Fusarium_neocosmosporiellum_Guinea_Arachis_hypogaea
Ambrosia
Fusarium Clade
Clade A
Clade B
0.0100

Fig. 3. Multilocus phylogenetic analysis of the species in the Ambrosia *Fusarium* Clade (AFC) using combined sequences from the ITS, TEF1-α, and RPB2 gene regions. The phylogram was constructed using maximum likelihood with 1000 bootstrap replicates. Isolates in bold were sequenced in this study. Two early diverging monophyletic sister clades are identified as Clade A and B. The highlighted boxes indicate the 19 species within the AFC and are identified as AF-1 through to AF-19 using an ad hoc nomenclature (Na et al. 2018; Carrillo et al. 2019). The new species in this study, *Fusarium rekanum* is represented by AF-19. The beetle vector of the AFC fusaria is indicated where known. *Fusarium neocosmosporiellum* (NRRL22468) represents the outgroup. T represents ex-type cultures

Taxonomy

Based on morphological and molecular evidence, the *Fusarium* isolates from *E. perbrevis* mycangia and brood galleries collected from infested *A. crassicarpa,* represent a novel associate of the TSHBa beetle. It is consequently described as follows:

Fusarium rekanum sp. nov. Lynn & Marinc. (Figs. 3, 4).

MycoBank (MB 831926).

Etymology The name *rekanum* is derived from the Bahasa Indonesia word "rekan" meaning associate and reflects the relationship between the fungus and its beetle vector, *E. perbrevis*.

Culture characteristics Colony colour on PDA at 25 °C for 14 days in dark white to buff (pale yellow). Colony margin smooth and colony elevation raised to umbonate. Reverse pigmentation pale luteous to luteous. Odour of yeast or brewing beer. Exudates absent. Colonies on PDA in dark radial mycelial growth rates of an average of 2.49 mm/day at 15 °C, 4.94 mm/day at 20 °C, 7.66 mm/day at 25 °C, 7.52 mm/day at 30 °C and 0.9 mm/day at 35 °C. *Conidial pustules*, produced on sporodochia, formed on older cultures grown on PDA, pale luteous to saffron, luteous to sienna, and ochreous. *Aerial mycelium* sparse with occasional pionnotal colony appearance, or developed abundantly, loose to floccose, white. *Chlamydospores* formed abundantly in hyphae, rarely in conidia, mostly round to oval, intercalary or terminal, single, paired, rarely clustered, or often in chains, hyaline, smooth, rarely rough-walled, 6–(7)–9.5–(11.5)–14.5 × 4–(7)–9–(11)–14 µm. *Sclerotia* absent. Sporulation on SNA abundant, particularly under UV light, retarded on PDA. *Sporodochia* formed sparsely on SNA, abundantly on PDA. *Aerial conidiophores* formed abundantly on SNA and PDA, erect, tall, thin walled and narrow with no tapering towards apex, mostly unbranched, 24–(49.5)–77.5–(105.5)–139.5 × 2–(4.5)–6–(7.5)–10 µm, forming monophialides integrated in apices. *Aerial phialides* simple, sub-cylindrical with slight bulging at midsection, with discreet collarette. *Aerial conidia* (1) mostly oval, two-celled oval to obovoid with truncated base, 0–1(–2)-septa, 7.5–(10)–13–(16)–18 × 3–(4.5)–5–(6)–7 µm, (2) falcate to clavate, slightly curved cylindrical, (0–)2–5(–6)-septate conidia, morphologically similar to the falcate to clavate sporodochial conidia. *Sporodochial conidiophores* thick, short and typically undulate, mostly unbranched or irregularly branched, forming apical monophialides. *Sporodochial phialides* simple, curved or crooked tube shaped, with discreet collarette. *Sporodochial conidia* (1) hyaline, mostly curved clavate, swollen in upper parts, tapering toward the base, often with a round, blunt or occasionally slightly papillate apical cell, with a barley notched distinct foot–like basal cell, (0–)2–6 (–6)-septate, formed on PDA and SNA, 33–(36)–40–(44)–48 × 6.5–(7)–8.5–(9.5)–11.5 µm, (2) obovoid or short-clavate to pyriform, curved or straight conidia, with a rounded apex and truncate base, (0–)1(–2)-septate, formed sometimes together with multi-septate conidia from sporodochial conidiophores, particularly on PDA.

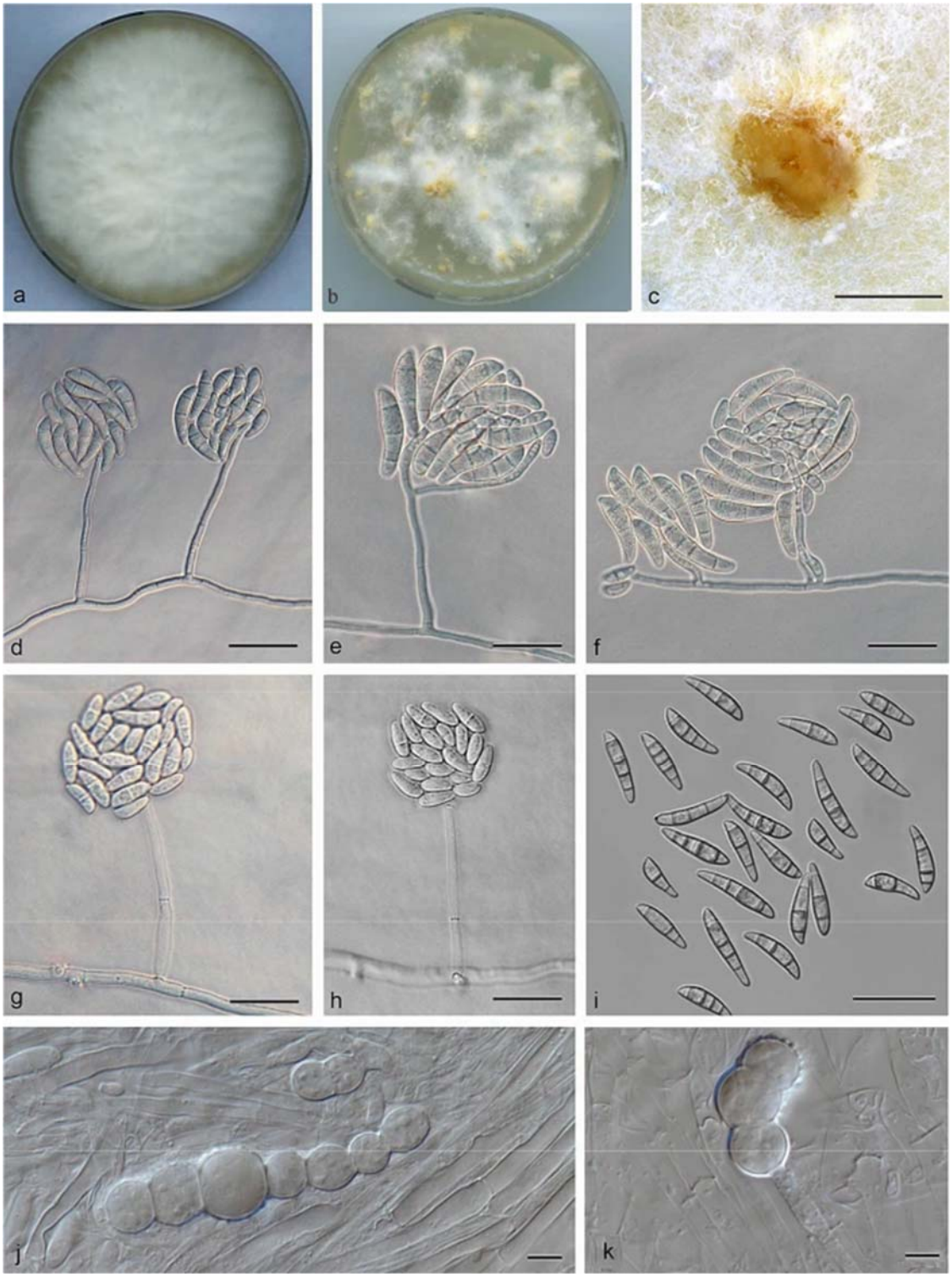

Fig. 4. Morphological characteristics of *Fusarium rekanum* (ex-type CMW 52862 = PPRI 27163) on PDA and SNA. **a**–**c**, **i** Morphology of *F. rekanum* cultures grown on potato dextrose agar (PDA), **d**–**h**, **j**–**k** morphology of 14-day-old *F. rekanum* cultures grown on synthetic low-nutrient agar (SNA). **a**. Colony morphology on PDA at 2 weeks. **b**, **c** White-buff conidial masses formed in culture on PDA after 1 month. **d**–**h** Simple to branched aerial conidiophores forming 0-multiseptate conidia, often swollen apically with 1–5 septa or oval to short clavate with 0–1 septa. **i** Multiseptate sporodochial conidia with a round, blunt apical cell, and a barley notched distinct foot-like basal cell with 4–5 septa. **j**–**k** Round to oval chlamydospores, in chains, formed intercalary or terminally in hyphae. Scale bars: c = 2 mm, d–i = 30 µm, j–k = 5 µm

Habitat Acacia crassicarpa plantations infested with ambrosia beetles in Riau, Indonesia.

Distribution Riau, Indonesia.

Specimen examined Indonesia, Riau, Pelalawan, *Acacia crassicarpa* plantation, isolated from *A. crassicarpa* infested with *E. perbrevis* (TSHBa), April 2017, K. M. T. Lynn, HOLOTYPE PREM 62333, living culture ex-type CMW 52862 = PPRI 27163.

Additional specimens Indonesia, Riau, Pelalawan, *A. crassicarpa* plantation, isolated from a mycangium of *E. perbrevis* (TSHBa). November 2018, K. M. T. Lynn, PREM 62334, living culture CMW 53688 = PPRI 27165; PREM 62335, living culture CMW 53691 = PPRI 27164.

Notes: Fusarium rekanum resembles *Fusarium* spp. residing in the clade that accommodates the associates of *Euwallacea* spp., particularly *F. euwallaceae*, *F. kuroshium*, and *F. ambrosium*, in various morphological features. It differs from *F. euwallaceae*, *F. kuroshium* and *F. ambrosium* in producing very few rough-walled chlamydospores formed on conidia. *Fusarium rekanum* also differs from both *F. euwallaceae* and *F. kuroshium* in the pigmentation of the conidial pustules, which are lighter in colour on PDA, and the lack of pigmented sporodochial conidia. *Fusarium kuroshium* has darker colonies after 14 days when compared to *F. rekanum*.

Fig. 5. Lesions formed on seven to eight-month-old *Acacia crassicarpa* trees inoculated with a control and with *Fusarium rekanum* after a 30-day incubation period. **a** Wound response of *A. crassicarpa* inoculated with the control. **b** Red lesions on *A. crassicarpa* inoculated with CMW 52862 (Treatment 1)

Pathogenicity assay

The *A. crassicarpa* trees inoculated with the two isolates of *F. rekanum* sp. nov, showed no external signs of disease after 30 days. However, red-coloured lesions, that were absent in the control inoculation, were observed around the inoculation sites, underneath the bark (Fig. 5). *Acacia crassicarpa* inoculated with isolate CMW 52862 (Treatment 1) produced lesions with a mean length of 8.2 ± 4.8 cm and *A. crassicarpa* inoculated with isolate CMW 51764 (Treatment 2) produced lesions with a mean length of 13.9 ± 7.6 cm. Trees treated with sterile agar plugs as controls produced wound response lesions having a mean length of 5.2 ± 1.6 cm. Mean lesion lengths associated with isolate CMW 51764 (Treatment 2) were found to be significantly larger than the controls ($P < 0.05$). Isolate CMW 52862 (Treatment 1) did not produce significantly longer lesions when compared to the negative control ($P > 0.05$) (Fig. 6).

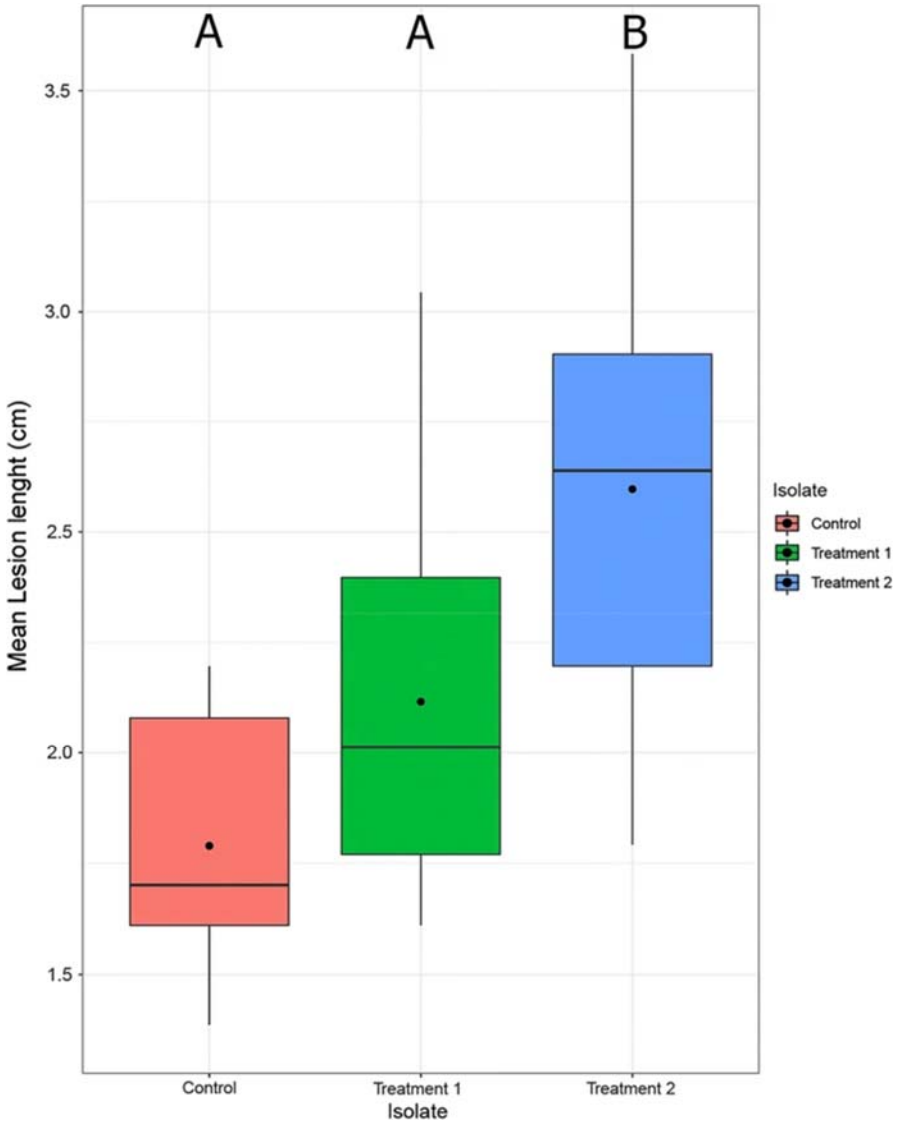

Fig. 6. Statistical variance and mean of log transformed lesion lengths (cm) on inoculated *A. crassicarpa*, represented in a boxplot. Based on the ad hoc Tukey's bootstrap test, Treatment 1 (CMW 52862) is not significantly different from the control as denoted by (A). Treatment 2 (CMW 51764) is the only treatment that is significantly different, both from the control and from treatment 2 (B)

The TEF1-α sequences generated for the cultures re-isolated from the lesions, aligned perfectly to the TEF1-α sequence data for the isolates (CMW 52862 and CMW 51764) used for the inoculations. Isolations from the stained margins of the lesions (wound response) associated with the control inoculations yielded only secondary contaminant fungi.

Discussion

Based on morphological and molecular characteristics, the results of this study show that *E. perbrevis* (the Tea Shot Hole Borer a) is the most commonly encountered beetle infesting healthy *A. crassicarpa* trees in the sampled areas of Riau, Indonesia. This beetle was identified following the recent taxonomic revision of Smith et al. (2019), that included the same species collected in East Java, Indonesia. The dominant fungal associate of this beetle was identified as a new AFC *Fusarium* species, described here as *F. rekanum* sp. nov. A preliminary inoculation trial with *F. rekanum* sp. nov. showed that the fungus is able to cause lesions but that it is likely not an aggressive pathogen on *A. crassicarpa*.

Specimens collected across multiple geographically separated compartments, at varying time points and on trees of different ages, show that *E. perbrevis* is a common pest on the sampled, non-native *A. crassicarpa* in Riau, Indonesia. This is the same species that has previously been treated in the aggregate species *E. fornicatus* (Smith et al. 2019), and that is believed to be native to the area. The common occurrence of this beetle over a relatively wide distribution suggests that they have migrated from the natural forests into the *A. crassicarpa* plantations.

Fusarium rekanum could be distinguished as a novel lineage, separate from the 18 other previously identified *Fusarium* spp. (AFC species) associated with *Euwallacea* spp. (Carrillo et al. 2019) based on multilocus phylogenetic inference. The invasive haplotype (H8) of *E. perbrevis* (TSHBa), has recently been shown to vector five members (AF-1, AF-13, AF-14, AF-17, AF-18) of the AFC (Carrillo et al. 2019). Thus far, only *F. ambrosium* (AF-1) has been formally described (Gadd and Loos 1947; Kasson et al. 2013), while the remaining four taxa (AF-13, 14, 17, 18), originating from Taiwan, have yet to be named (Carrillo et al. 2019). None of these AFC members were isolated from *E. perbrevis* mycangia or corresponding brood galleries such as those analysed in the present study. Our phylogenetic analysis suggests that *F. rekanum* is relatively distantly related to these other AFC members (Fig. 3). Because *F. rekanum* is the only species thus far described from Indonesia, this could reflect the geographic origins, plant hosts, and different haplotypes of the *Euwallacea* beetles from which the fungi were isolated.

The two isolates of *F. rekanum* tested for pathogenicity in this study resulted in lesions, but these were relatively small, and similar to those produced in the control inoculated *A. crassicarpa*. This implies that the fungus has a low level of aggressiveness, although this was a preliminary study including only a small number of trees. Future studies including a greater number of isolates would be required to better understand whether the fungus might play a role in tree decline. Therefore, it is possible that this species is purely involved in providing nutrition for its beetle symbiont (Beaver 1989; Farrell et al. 2001).

Currently, the damage observed on *A. crassicarpa* appears to be the combination of the mechanical damage caused by mass attack of beetles, and the repeated inoculation of the weakly pathogenic *Fusarium* sp. The contribution, if any, of the other fungi isolated in this study (Supplementary Table 1), in the observed tree decline would also need to be further

investigated. This would especially be true for the *Graphium* sp. and *Paracremonium* sp. as they have previously been shown to play an important role in the development and establishment of their beetle hosts (Lynch et al. 2016).

Mass accumulation of a variety of ambrosia beetles in a host can occur over a period of months, with multiple species coexisting in the same habitat (Carrillo et al. 2014). In the present study, five different beetle species were found in moderately infested tree hosts. However, as South East Asia is believed to be the native range of many species of the Xyleborini (Hulcr et al. 2015), it is possible that many more species of ambrosia beetle and their associated fungi could infest *A. crassicarpa*. This overlap in gallery occupation by different ambrosia beetle species, may give rise to lateral transmission of the associated fungi between different beetle species (Ploetz et al. 2017). How specific these beetle and fungal associations are, and whether *F. rekanum* is obligately required for the survival and development of *E. perbrevis*, remains to be determined.

The extensive native range of species in the *E. fornicatus* species complex and the results of phylogenetic analyses presented here, and in previous studies on these insects, suggests that there is substantial biological variation among native populations of *E. perbrevis* and their *Fusarium* spp. associates (Gomez et al. 2018; Smith et al. 2019). Consistent with a recent study by Carrillo et al. (2019), we hypothesise that a promiscuous relationship exists between members of the *E. fornicatus* complex and *Fusarium* spp., in areas where these organisms are native. This is in contrast to the strict symbiosis observed in non-native areas (O'Donnell et al. 2015; Stouthamer et al. 2017).

Acknowledgements

This study was initiated through the bilateral agreement between the Forestry and Agricultural Biotechnology Institute (FABI) and the April Group, RGE, Indonesia. We acknowledge members of Tree Protection and Cooperation Programme (TPCP) and the National Research Foundation (NRF, SFH170527234109), South Africa for financial support. We thank Darryl Herron, Arista Fourie, Joey Hulbert, Wilma Nel and members of the April Group, RGE, Indonesia, particularly Pantun David Mangatas Lumban Gaol and Hengki Marantika, for their technical assistance. Two anonymous reviewers provided valuable input that enabled us to improve the original manuscript, for which we are grateful.

References

Aoki T, O'Donnell K, Scandiani MM (2005) Sudden death syndrome of soybean in South America is caused by four species of *Fusarium*: *Fusarium brasiliense* sp. nov., *F. cuneirostrum* sp. nov., *F. tucumaniae*, and *F. virguliforme*. Mycoscience 46:162–183. https://doi.org/10.1007/s10267-005-0235-y

Aoki T, Kasson M, Berger MC et al (2018) *Fusarium oligoseptatum* sp. nov., a mycosymbiont of the ambrosia beetle *Euwallacea validus* in the Eastern U.S. and typification of *F. ambrosium*. Fungal Syst Evol 1:13–22. https://doi.org/10.3114/fuse.2018.01.03

Aoki T, Smith JA, Kasson MT et al (2019) Three novel Ambrosia *Fusarium* Clade species producing clavate macroconidia known (*F. floridanum* and *F. obliquiseptatum*) or predicted (*F. tuaranense*) to

be farmed by *Euwallacea* spp. (Coleoptera: Scolytinae) on woody hosts. Mycologia 11:1–17. https://doi.org/10.1080/00275514.2019.1647074

Batra LR (1963) Ecology of ambrosia fungi and their dissemination by beetles. Kansas Acad Sci 66:213–236. https://www-jstor-org.uplib.idm.oclc.org/stable/3626562

Beaver RA (1989) Insect-Fungus relationships in the bark and ambrosia beetles. Beetle-Fungus Assoc. https://doi.org/10.1016/b978-0-12-751800-8.50011-2

Boland JM, Woodward DL (2019) Impacts of the invasive shot hole borer (*Euwallacea kuroshio*) are linked to sewage pollution in southern California: the enriched tree hypothesis. PeerJ 7:1–22. https://doi.org/10.7717/peerj.6812

Carrillo D, Duncan RE, Ploetz JN et al (2014) Lateral transfer of a phytopathogenic symbiont among native and exotic ambrosia beetles. Plant Pathol 63:54–62. https://doi.org/10.1111/ppa.12073

Carrillo JD, Rugman-Jones PF, Husein D et al (2019) Members of the *Euwallacea fornicatus* species complex exhibit promiscuous mutualism with ambrosia fungi in Taiwan. Fungal Genet Biol 133:1–12. https://doi.org/10.1016/j.fgb.2019.103269

Cognato AI, Hoebeke ER, Kajimura H, Smith SM (2015) History of the exotic ambrosia beetles *Euwallacea interjectus* and *Euwallacea validus* (Coleoptera: Curculionidae: Xyleborini) in the United States. J Econ Entomol 108:1129–1135. https://doi.org/10.1093/jee/tov073

Darriba D, Taboada GL, Doallo R, Posada D (2015) jModelTest 2: more models, new heuristics and high-performance computing. Eur PMC Funders Gr 9:6–9. https://doi.org/10.1038/nmeth.2109.jmodeltest

de Mendiburu F (2019) Agricolae: statistical procedures for agricultural research version 1.2-8. http://tarwi.lamolina.edu.pe/~fmendiburu)

Edgar RC (2004) MUSCLE: multiple sequence alignment with high accuracy and high throughput. Nucleic Acids Res 32:1792–1797. https://doi.org/10.1093/nar/gkh340

Eskalen A, Stouthamer R, Lynch SC et al (2013) Host range of Fusarium dieback and its ambrosia beetle (Coleoptera: Scolytinae) vector in southern California. Plant Dis 97:938–951. https://doi.org/10.1094/pdis-11-12-1026-re

Farrell BD, Sequeira AS, Meara BCO et al (2001) The evolution of agriculture in beetles (Curculionidae: Scolytinae and Platypodinae). J Evol 55:2011–2027. https://doi.org/10.1111/j.0014-3820.2001.tb01318.x

Folmer O, Black M, Hoeh W et al (1994) DNA primers for amplification of mitochondrial cytochrome c oxidase subunit I from diverse metazoan invertebrates. Mol Mar Biol Biotechnol 3:294–299

Freeman S, Sharon M, Maymon M et al (2013) *Fusarium euwallaceae* sp. nov.—a symbiotic fungus of *Euwallacea* sp., an invasive ambrosia beetle in Israel and California. Mycologia 105:1595–1606. https://doi.org/10.3852/13-066

Gadd CH, Loos CA (1947) The ambrosia fungus of *Xyleborus fornicatus* Eich. Trans Br Mycol Soc 31:13–19. https://doi.org/10.1016/s0007-1536(47)80003-8

Gomez DF, Skelton J, Steininger MS et al (2018) Species delineation within the *Euwallacea fornicatus* (Coleoptera: Curculionidae) complex revealed by morphometric and phylogenetic analyses. Insect Syst Divers 2:1–11. https://doi.org/10.1093/isd/ixy018

Guindon S, Dufayard J, Lefort V (2010) New algorithms and methods to estimate maximum-likelihood phylogenies: assessing the performance of PhyML 3.0. Syst Biol 59(3):307–321

Harrington TC, McNew D, Mayers C et al (2014) *Ambrosiella roeperi* sp. nov. is the mycangial symbiont of the granulate ambrosia beetle, *Xylosandrus crassiusculus*. Mycologia 106:835–845. https://doi.org/10.3852/13-354

Hughes MA, Riggins JJ, Koch FH et al (2017) No rest for the laurels: symbiotic invaders cause unprecedented damage to southern USA forests. Biol Invasions 19:2143–2157. https://doi.org/10.1007/s10530-017-1427-z

Hulcr J, Dunn RR (2011) The sudden emergence of pathogenicity in insect-fungus symbioses threatens naive forest ecosystems. Proc R Soc B Biol Sci 278:2866–2873. https://doi.org/10.1098/rspb.2011.1130

Hulcr J, Atkinson TH, Cognato AI et al (2015) Morphology, taxonomy, and phylogenetics of bark beetles. In: Bark beetles: biology and ecology of native and invasive species. Elsevier Inc., pp 41–84

Hulcr J, Black A, Prior K et al (2017) Studies of ambrosia beetles (Coleoptera: Curculionidae) in their native ranges help predict invasion impact. Florida Entomol 100:257–261. https://doi.org/10.1653/024.100.0219

Jacobs K, Bergdahl DR, Wingfield MJ et al (2004) *Leptographium wingfieldii* introduced into North America and found associated with exotic *Tomicus piniperda* and native bark beetles. Mycol Res 108:411–418. https://doi.org/10.1017/s0953756204009748

Jordal BH, Sequeira AS, Cognato AI (2011) The age and phylogeny of wood boring weevils and the origin of subsociality. Mol Phylogenet Evol 59:708–724. https://doi.org/10.1016/j.ympev.2011.03.016

Kajimura H, Hijii N (1992) Dynamics of the fungal symbionts in the gallery system and the mycangia of the ambrosia beetle, *Xylosandrus mutilatus* (Blandford) (Coleoptera: Scolytidae) in relation to its life history. Ecol Res 7:107–117. https://doi.org/10.1007/bf02348489

Kasson MT, O'Donnell K, Rooney AP et al (2013) An inordinate fondness for *Fusarium*: Phylogenetic diversity of *fusaria* cultivated by ambrosia beetles in the genus *Euwallacea* on avocado and other plant hosts. Fungal Genet Biol 56:147–157. https://doi.org/10.1016/j.fgb.2013.04.004

Kirkendall LR, Biedermann PHW, Jordal BH (2015) Evolution and diversity of bark and ambrosia beetles. In: Bark beetles: biology and ecology of native and invasive species. Elsevier Inc., pp 85–156

Kück P, Longo GC (2014) FASconCAT-G: extensive functions for multiple sequence alignment preparations concerning phylogenetic studies. Front Zool 11:1–8

Kumar S, Stecher G, Tamura K (2016) MEGA7: molecular evolutionary genetics analysis version 7.0 for bigger datasets. Mol Biol Evol 33:1870–1874. https://doi.org/10.1093/molbev/msw054

Kurtzman CP, Robnett CJ (1997) Identification of clinically important ascomycetous yeasts based on nucleotide divergence in the 5′ end of the large-subunit (26S) ribosomal DNA gene. J Clin Microbiol 35:1216–1223

Leslie JF, Summerell BA (2006) The *Fusarium* laboratory manual

Lynch SC, Twizeyimana M, Mayorquin JS et al (2016) Identification, pathogenicity and abundance of *Paracremonium pembeum* sp. nov. and *Graphium euwallaceae* sp. nov.—two newly discovered mycangial associates of the polyphagous shot hole borer (*Euwallacea* sp.) in California. Mycologia 108:313–329. https://doi.org/10.3852/15-063

Miller MA, Pfeiffer W, Schwartz T (2010) Creating the CIPRES science gateway for inference of large phylogenetic trees. 2010 Gatew Comput Environ Work GCE 2010. https://doi.org/10.1109/gce.2010.5676129

Mueller UG, Gerardo NM, Aanen DK et al (2005) The evolution of agriculture in insects. Annu Rev Ecol Evol Syst 36:563–595. https://doi.org/10.1146/annurev.ecolsys.36.102003.152626

Na F, Carrillo JD, Mayorquin JS et al (2018) Two novel fungal symbionts *Fusarium kuroshium* sp. nov. and *Graphium kuroshium* sp. nov. of Kuroshio shot hole borer (*Euwallacea* sp. nr. *fornicatus*) cause Fusarium Dieback on woody host species in California. Plant Dis 102:1154–1164. https://doi.org/10.1094/pdis-07-17-1042-re

O'Donnell K, Cigelnik E (1997) Two divergent intragenomic rDNA ITS2 types within a monophyletic lineage of the fungus *Fusarium* are nonorthologous. Mol Phylogenet Evol 7:103–116. https://doi.org/10.1006/mpev.1996.0376

O'Donnell K, Kistler HC, Cigelnik E, Ploetz RC (1998) Multiple evolutionary origins of the fungus causing Panama disease of banana: concordant evidence from nuclear and mitochondrial gene genealogies. Proc Natl Acad Sci 95:2044–2049. https://doi.org/10.1073/pnas.95.5.2044

O'Donnell K, Sarver BAJ, Brandt M et al (2007) Phylogenetic diversity and microsphere array-based genotyping of human pathogenic *fusaria*, including isolates from the multistate contact lens-associated U.S. keratitis outbreaks of 2005 and 2006. J Clin Microbiol 45:2235–2248. https://doi.org/10.1128/jcm.00533-07

O'Donnell K, Sutton DA, Rinaldi MG et al (2010) Internet-accessible DNA sequence database for identifying fusaria from human and animal infections. J Clin Microbiol 48:3708–3718. https://doi.org/10.1128/jcm.00989-10

O'Donnell K, Sink S, Libeskind-Hadas R et al (2015) Discordant phylogenies suggest repeated host shifts in the *Fusarium-Euwallacea* ambrosia beetle mutualism. Fungal Genet Biol 82:277–290. https://doi.org/10.1016/j.fgb.2014.10.014

O'Donnell K, Libeskind-Hadas R, Hulcr J et al (2016) Invasive Asian *Fusarium – Euwallacea* ambrosia beetle mutualists pose a serious threat to forests, urban landscapes and the avocado industry. Phytoparasitica 44:435–442. https://doi.org/10.1007/s12600-016-0543-0

Ploetz RC, Konkol JL, Narvaez T et al (2017) Presence and prevalence of *Raffaelea lauricola*, cause of laurel wilt, in different species of ambrosia beetle in Florida, USA. J Econ Entomol 110:347–354. https://doi.org/10.1093/jee/tow292

Ranger CM, Schultz PB, Frank SD et al (2015) Non-native ambrosia beetles as opportunistic exploiters of living but weakened trees. PLoS ONE 10:1–21. https://doi.org/10.1371/journal.pone.0131496

Roy K, Ewing CP, Hughes MA et al (2018) Presence and viability of *Ceratocystis lukuohia* in ambrosia beetle frass from Rapid 'Ōhi'a death-affected *Metrosideros polymorpha* trees on Hawai'i Island. For Pathol. https://doi.org/10.1111/efp.12476

Sandoval-Denis M, Lombard L, Crous PW (2019) Back to the roots: a reappraisal of *Neocosmospora*. Persoonia - Mol Phylogeny Evol Fungi 43(1):90–185. https://doi.org/10.3767/persoonia.2019.43.04

Skelton J, Jusino MA, Carlson PM et al (2019) Relationships among wood-boring beetles, fungi, and the decomposition of forest biomass. Mol Ecol 28:4971–4986. https://doi.org/10.1111/mec.15263

Smith SM, Gomez DF, Beaver RA et al (2019) Reassessment of the species in the *Euwallacea Fornicatus* (Coleoptera: Curculionidae: Scolytinae) complex after the rediscovery of the "lost" type specimen. Insects 10:1–11. https://doi.org/10.3390/insects10090261

Stamatakis A (2014) RAxML version 8: a tool for phylogenetic analysis and post-analysis of large phylogenies. Bioinformatics 30:1312–1313. https://doi.org/10.1093/bioinformatics/btu033

Stouthamer R, Rugman-Jones P, Thu PQ et al (2017) Tracing the origin of a cryptic invader: phylogeography of the *Euwallacea fornicatus* (Coleoptera: Curculionidae: Scolytinae) species complex. Agric For Entomol 19:366–375. https://doi.org/10.1111/afe.12215

White TJ, Bruns T, Lee S, Taylor J (1990) Amplification and direct sequencing of fungal ribosomal RNA genes for phylogenetics. PCR Protoc 315–322. https://doi.org/10.1016/b978-0-12-372180-8.50042-1

Wickham H (2017) Welcome to the tidyverse. J Open Source Softw 4:43. https://doi.org/10.21105/joss.01686